Treatment of highly turbid water in disaster conditions using coagulation-flocculation process: modeling and optimization

Danial Nayeri and Seyyed Alireza Mousavi

ABSTRACT

In the present research, the coagulation-flocculation (CF) process was used to eliminate highly turbid water in disaster conditions. To better understand the efficiency of the system, the impact of various numerical factors namely; initial turbidity (10–350 NTU), pH (5–9), coagulant dosage (50–250 mg/L), rapid mixing (120–280 rpm), slow mixing (30–50 rpm), and sedimentation time (10–50 min) were optimized through the central composite design (CCD) under response surface methodology (RSM). Based on analysis of variance (ANOVA), the quadratic model was more suitable for the dataset with $R^2 = 0.85$ for removing turbidity. Moreover, the results of the present study revealed that the highest turbidity removal (99.14%) was observed at pH (9), alum dosage (50 mg/L), initial turbidity (350 NTU), rapid mixing (280 rpm), slow mixing (50 rpm), and sedimentation time (50 min). Furthermore, the residual turbidity at the maximum efficiency of the system was 3 NTU.

Key words | coagulation, disaster, drinking water, optimization, turbidity

Danial Nayeri
Seyyed Alireza Mousavi (corresponding author)
Department of Environmental Health Engineering,
School of Public Health, and Research Center for Environmental Determinants of Health (RCEDH),
Health Institute,
Kermanshah University of Medical Sciences,
Kermanshah,
Iran
E-mail: *seyyedarm@yahoo.com*

Danial Nayeri
Student research committee,
Kermanshah University of Medical Sciences,
Kermanshah,
Iran

Seyyed Alireza Mousavi
Social Development and Health Promotion Research Center,
Kermanshah University of Medical Sciences,
Kermanshah,
Iran

HIGHLIGHTS

- This study has been performed and designed to investigate the efficiency of commercial aluminum sulfate as an efficient coagulant for the removal of turbidity with high concentrations to simulate crises in water resources.
- Also, the effect of main variables; pH, alum dosage, rapid and slow mixing, and sedimentation time on the process has been optimized and an empirical model has been developed.

INTRODUCTION

Over the past decades, disasters, especially floods and earthquakes, have had adverse effects on water quality such as increasing suspended solids (SS) and colloids more than the standard range (Ang *et al.* 2016). Among the various water quality indicators, turbidity is one of the most significant indicators for detecting freshwater characteristics (Antov *et al.* 2018). Typically, the drinking water-based on turbidity value can be divided into four categories as follows: low turbidity (less than 50 NTU), medium turbidity (50–100 NTU), high turbidity (100–200 NTU), and very high turbidity (more than 300 NTU) (Altaher 2012). Excessive turbidity in drinking water can also be associated with the presence of organic materials, dye, and microorganisms such as viruses, and certain bacteria, therefore, it increases the health and environmental concerns (Aboubaraka *et al.* 2017; Al-Husseini *et al.* 2018).

Based on the above reasons, the World Health Organization (WHO) proposed that acceptable levels of turbidity in drinking water must be less than 5 NTU (Al-Husseini *et al.* 2018). Therefore, to achieve WHO standards various chemical-physical technologies such as sequencing batch reactor (SBR) (Azimi *et al.* 2019), ceramic membranes (Park *et al.*

doi: 10.2166/wqrj.2020.120

2020), ozonation (Hajiali & Pirumyan 2014), and coagulation (Zhang *et al.* 2018) have been used for removing turbidity from water. Among them, the coagulation–flocculation (CF) process is the most reliable technology to reduce any pollutants (turbidity, particulates, and organic matters) from drinking water (Zhao *et al.* 2012).

Previous studies confirmed that the CF process has been extensively applied in water treatment plants (WTPs) because of its superior properties such as simplicity, cost-effectiveness, high efficiency, non-toxic method, and low energy consumption (Lim *et al.* 2018; Ozairi *et al.* 2020). Typically, the CF process has been performed by using various coagulants such as iron-aluminum salts, and long-chain polymers for the removal of turbidity from raw water (Baruth 2005). Previous works indicated that aluminum salts (alum) with a chemical formula ($Al_2(SO_4)3.18H_2O$) has a better potential for the removal of turbidity than ferric salts. However, alum cost is higher than ferric chloride (Gobena *et al.* 2018; Kumari & Gupta 2020). Studies have shown that there is a direct correlation between the use of alum and neuropathological diseases such as Alzheimer's (Huang *et al.* 2015). Therefore, it is necessary to optimize the main factors such as coagulant dosage, mixing speed, effluent pH, temperature, and time, which have a direct effect on the CF process (Corral Bobadilla *et al.* 2019).

In recent years, several methods such as an artificial neural network (ANN) (Singh & Gupta 2012), adaptive neuro-fuzzy inference system (ANFIS) (Kim & Parnichkun 2017), multi-layer perceptron (MLP) (Gagnon *et al.* 1997), generalized regression neural network (GRNN) (Specht 1991), and response surface methodology (RSM) (Corral Bobadilla *et al.* 2019) have been applied for modeling and optimization of the CF process. Among the aforementioned methods, RSM as a statistical method has been widely used for analyzing, modeling, and optimizing the effect of different variables and their responses on the system (Corral Bobadilla *et al.* 2019). Furthermore, it can be used in various systems to obtain maximum performance with the ability to decrease the number of examinations (Singh & Kumar 2020).

Muyibi & Alfugara (2003) used alum and Moringa oleifera seed as coagulants for the removal of turbidity from water at different levels; low turbidity (21.5–49.3 NTU), moderate turbidity (51.8–114 NTU) and high turbidity (163–494 NTU). Their results showed that the process can achieve the minimum residuals of turbidity, 1.4, 1.9, and 0.9 NTU, using Moringa oleifera, alum, and alum with Moringa oleifera, respectively (Muyibi & Alfugara 2003). Another study by Baghvand *et al.* (2010) reported that the highest turbidity removal by using alum and ferric chloride as coagulant was 82.9–99.0 and 92.9–99.4%, respectively (Baghvand *et al.* 2010). Agbovi & Wilson (2019) examined and optimized the removal efficiency of turbidity using an amphoteric chitosan-based flocculant–ferric chloride by RSM. They found that the turbidity removal under optimum conditions was 96.7%. Furthermore, the results showed that the process is highly dependent on the pH, $FeCl_3$ dosage, and the flocculant dosage (Agbovi & Wilson 2019). Usefi & Asadi-Ghalhari (2019) used the coagulation–flocculation process in the elimination of turbidity using rice starch and the system was optimized using the central composite design (CCD) approach. The results demonstrated that 98.4% of turbidity was removed at the optimal point. Moreover, they showed that among the four independent variables (pH, settling time, rice starch dosage, and slow mixing), pH had the most significant effect on the turbidity removal (Usefi & Asadi-Ghalhari 2019).

Therefore, due to the importance of optimizing the coagulant factors, herein, the influences of operational parameters (coagulant dose and pH, rapid mixing, slow mixing, and sedimentation time) on the removal of turbidity were investigated using the CCD-RSM method. Furthermore, this is the first study that has completely described the role of rapid mixing; slow mixing on the coagulation-flocculation process.

MATERIALS AND METHODS

Chemicals

Commercial aluminum sulfate ($Al_2(SO_4)_3{\cdot}14H_2O$; 17%), with a molecular weight (M_W) of 342.15 g/mol was purchased from Goglagh Company, Iran. All reagents with high analytical grade were purchased from Merck Company, Germany.

Turbid water preparation

To prepare turbid water in desired turbidities, clay soil (without any modification) from the suburb of Kermanshah city

was collected and dried at 150 °C for 150 min using an oven (Memmert 854, Germany). The synthetic turbid water was prepared daily using 10 g of dried clay soil in 2 L of tap water and mixed at 30 rpm for 1 hour to complete hydration of the particles. Consequently, the desired range of turbid water (10–350 NTU) was prepared using the stock solution.

Coagulation–flocculation experiment

The CF process was performed using a Jar test apparatus (AQUALYTIC, Germany) with six beakers (1,000 mL working volume). The jar test was conducted at three stages: coagulation (rapid mixing; 120–280 rpm for 1 min), flocculation (slow mixing; 30–50 rpm for 20 min), and sedimentation at different settling times (10–50 min). At the beginning of the process, all beakers were filled with turbid water with initial turbidity of 10–350 NTU and then alum at desired dosages (50–250 mg/L) was added into the solutions. The solution pH was adjusted to the desired values of 5–9 using sodium hydroxide (NaOH) and sulfuric acid (H_2SO_4) using a pH meter (WTW, Germany). The rapid and slow mixing was conducted subsequently based on Table 1. After the end of the process, sampling was carried out from 2 to 3 cm under the surface of the solution. The residual of turbidity was analyzed using a turbidimeter (2100 p, HACH Company, USA). The efficiency of the system was calculated according to Equation (1) (Lim *et al.* 2018):

$$\text{Turbidity removal } (\%) = \frac{C_0 - C}{C_0} \times 100 \quad (1)$$

Table 1 | The level of independent variables

Variables	Unit	Symbols	Coded levels		
			Low	Centre	High
Initial turbidity	NTU	A	10	180	350
Coagulant dosage	mg/l	B	50	150	250
Rapid mixing (RM)	rpm	C	120	200	280
Slow mixing (SM)	rpm	D	30	40	50
pH	–	E	5	7	9
Settling time (ST)	min	F	10	30	50

Experimental design and data analysis

The Design-Expert software (version 11.0.0.1) was used for optimization and data analysis of the experiments. The standard response surface methodology design known as central composite design was used to design experiments, model the data, and finally predict the responses (Mousavi *et al.* 2017; Aydar 2018). Moreover, RSM can optimize the process parameters with a minimum number of tests (Aydar 2018; Nayeri *et al.* 2019). ANOVA (analysis of variance) was used for data analysis and to develop a mathematical model (Momeni *et al.* 2018). Besides, the probability value (*P*-value) at a 95% confidence interval was used to evaluate the significance of model terms (Corral Bobadilla *et al.* 2019; Mousavi & Ibrahim 2016). The CCD is based on independent parameters such as: A: initial turbidity, B: alum dosage, C: rapid mixing, D: slow mixing, E: pH, and F: settling time at three levels (low, center points, and high level) (Table 1). Furthermore, the results of the experiments based on 86 runs are summarized in Table 2. The residual value of turbidity (Y1) based on NTU and removal efficiency served as output responses (Equation (2)). The predicting of optimal conditions was carried out based on the following developed model (Equation (2)) (Mousavi *et al.* 2019; Shahbazi *et al.* 2020):

$$Y = \beta_0 + \sum_{i=1}^{k} \beta_i x_i + \sum_{i=1}^{k} \beta_{ii} x_i^2 + \sum_{i<j}^{k} \sum \beta_{ij} x_i x_j + e \quad (2)$$

RESULTS AND DISCUSSION

Data analysis and modeling

The results of the ANOVA are shown in Table 3. According to the table, it is clear that terms such as A, B, D, E, F, AB, AE, AF, BF are significant (*P*-value < 0.05). The quality of model fitness (Equation (3)) was investigated by the R^2 coefficient (Noordin *et al.* 2004; Almasi *et al.* 2017), in which R^2 and adjusted R^2 were 0.8547 and 0.7871, respectively. The high adequate precision (greater than 4) and low coefficient of variation are attributed to the high accuracy and reliability of the proposed models (Zangeneh *et al.* 2016;

Table 2 | Experimental design for turbidity removal

	Parameters									Parameters							
Run no.	A (NTU)	B (mg/L)	C (rpm)	D (rpm)	E	F (min)	Final turbidity (NTU)	Removal %	Run no.	A (NTU)	B (mg/L)	C (rpm)	D (rpm)	E	F (min)	Final turbidity (NTU)	Removal %
1	180	150	200	40	7	30	75.5	57.1	44	350	50	120	30	9	50	4	98
2	350	50	120	50	9	10	7.3	97.91	45	350	250	120	30	9	50	3	99.14
3	180	150	200	40	7	30	50	71.59	46	10	250	280	50	9	50	5.8	47.27
4	180	150	200	40	7	30	46	74.44	47	10	50	280	30	9	10	3.4	66
5	350	250	280	30	9	10	6	98.28	48	10	50	280	30	5	10	9.9	10
6	350	250	120	50	5	10	69.4	8.17	49	180	150	200	40	7	30	64.4	63.4
7	350	250	120	50	5	50	27	92.28	50	350	50	280	30	9	10	8	97.71
8	180	150	200	35	7	30	7.37	95.94	51	10	250	280	30	5	50	5	50
9	350	50	120	50	5	50	20	94	52	350	250	280	50	9	10	33.1	90.54
10	10	250	120	30	9	50	3.5	98.11	53	180	150	200	45	7	30	68	61.33
11	350	50	280	50	9	50	3	99.14	54	350	250	280	50	5	10	57.5	83.57
12	180	150	200	40	8	30	55	69.44	55	350	50	280	50	5	10	64.5	81.57
13	10	250	120	50	5	10	25.4	–154	56	180	100	200	40	7	30	61.8	64.88
14	10	50	120	30	5	10	5	50	57	350	50	280	30	5	50	20.6	94.11
15	350	250	280	30	9	50	3.88	98.89	58	180	150	200	40	7	30	60	66.66
16	10	50	280	50	9	50	4.1	62.72	59	180	150	200	40	6	30	16.1	95.01
17	180	150	200	40	7	20	21.7	87.7	60	350	250	280	50	5	50	23	93.42
18	350	50	120	30	5	10	34	90	61	180	200	200	40	7	30	50	72.22
19	350	250	280	30	5	10	71	79.71	62	10	250	120	30	5	10	18.2	–82
20	350	50	120	50	5	10	62	80.28	63	265	150	200	40	7	30	18	93.2
21	95	150	200	40	7	30	21	78.89	64	10	250	280	50	5	10	22.1	–121
22	10	250	120	50	5	50	16.6	–66	65	10	50	120	30	5	50	4.54	54.04
23	180	150	200	40	7	30	65.4	62.8	66	350	250	120	30	9	10	12	96
24	10	250	120	50	9	50	5.18	52.9	67	10	50	280	30	5	50	6.37	36.3
25	10	250	280	30	9	50	2.46	77.63	68	350	50	120	50	9	50	25.6	92.68
26	10	250	120	30	9	10	21.9	–119	69	180	150	160	40	7	30	24	86.66
27	10	50	120	50	5	50	7.25	34.18	70	10	50	280	30	9	50	2.46	77.63
28	180	150	200	40	7	40	10.1	94.32	71	180	150	200	40	7	30	64	64.44
29	10	50	120	50	5	10	17.19	–71.9	72	350	250	120	30	5	50	14	96
30	350	50	280	30	9	50	3.2	99.08	73	10	250	280	30	5	10	11.4	–14

(*continued*)

Table 2 | continued

Run no.	Parameters A (NTU)	B (mg/L)	C (rpm)	D (rpm)	E	F (min)	Final turbidity (NTU)	Removal %	Run no.	Parameters A (NTU)	B (mg/L)	C (rpm)	D (rpm)	E	F (min)	Final turbidity (NTU)	Removal %
31	350	250	280	30	5	50	17.7	94.94	74	350	250	120	50	9	50	6.1	98.25
32	10	50	120	50	9	10	2.25	77.27	75	10	50	120	30	9	10	4	60
33	350	50	280	30	5	10	47	89.57	76	180	150	240	40	7	30	6.68	96.28
34	10	50	280	50	9	10	3	72.72	77	10	250	280	30	9	10	13	–30
35	180	150	200	40	7	30	61.8	64.88	78	10	50	120	30	9	50	4.28	56.68
36	10	50	280	50	5	10	5.3	51.8	79	10	50	280	50	5	50	8.3	24.54
37	350	50	280	50	5	50	22.1	93.68	80	180	150	200	40	7	30	58	67.22
38	10	250	120	50	9	10	21	–101	81	10	50	120	50	9	50	2.3	79.09
39	180	150	200	40	7	30	13.3	92.52	82	350	250	120	50	9	10	26.2	95.51
40	10	250	280	50	5	50	20	–100	83	350	50	280	50	9	10	7.1	97.97
41	350	50	120	30	5	50	13	96.2	84	10	250	280	50	9	10	19.7	–97
42	10	250	120	30	5	50	17.7	–77	85	350	250	120	30	5	10	50.7	85.51
43	350	50	120	30	9	10	7.1	97	86	350	250	280	50	9	50	7.6	97.88

Table 3 | Results of ANOVA

Source	Sum of squares	df	Mean square	F-value	*P*-value
Model	2.794×10^5	27	10,347.62	12.64	<0.0001
A	1.224×10^5	1	1.224×10^5	149.45	<0.0001
B	33,250.73	1	33,250.73	40.61	<0.0001
C	2,509.85	1	2,509.85	3.07	0.0853
D	6,595.31	1	6,595.31	8.06	0.0062
E	16,944.07	1	16,944.07	20.70	<0.0001
F	18,108.18	1	18,108.18	22.12	<0.0001
AB	25,767.47	1	25,767.47	31.47	<0.0001
AC	968.30	1	968.30	1.18	0.2813
AD	2,635.28	1	2,635.28	3.22	0.0780
AE	6,681.43	1	6,681.43	8.16	0.0059
AF	8,625.30	1	8,625.30	10.53	0.0019
BC	1,031.86	1	1,031.86	1.26	0.2662
BD	2,861.18	1	2,861.18	3.49	0.0666
BE	685.13	1	685.13	0.8368	0.3641
BF	9,786.65	1	9,786.65	11.95	0.0010
CD	50.41	1	50.41	0.0616	0.8049
CE	895.21	1	895.21	1.09	0.3001
CF	1,407.94	1	1,407.94	1.72	0.1949
DE	2,791.27	1	2,791.27	3.41	0.0699
DF	253.92	1	253.92	0.3101	0.5797
EF	567.63	1	567.63	0.6933	0.4085
A^2	7.91	1	7.91	0.0097	0.9220
B^2	589.86	1	589.86	0.7205	0.3995
C^2	125.79	1	125.79	0.1536	0.6965
D^2	75.09	1	75.09	0.0917	0.7631
E^2	9.64	1	9.64	0.0118	0.9140
F^2	110.32	1	110.32	0.1347	0.7149
Residual	47,486.60	58	818.73		
Pure error	844.86	9	93.87		
Cor total	3.269×10^5	85			

Nadarajan *et al.* 2018). Herein, adequate precision and CV values were 17.20 and 52.41, respectively. Based on the results, the quadratic model was more suitable for the dataset. Furthermore, the F-value of the model (12.64) confirmed the significance of the model. Based on Equation (3), the initial turbidity, settling time, pH, coagulant dosage, and rapid mixing had a positive and significant effect on turbidity removal.

Figure 1(a) illustrates that the predicted values of the model response are related to the observed values (real). Data points are fairly similar to each other and repetitive action is distributed. According to the results, this plot indicates that there is an acceptable correlation between the data obtained and the real evidence. The variation between the expected and the actual (residual) result is used to determine the accuracy (Gasemloo *et al.* 2019). Based on the aforementioned reasons, Figure 1(b) shows that the residuals are distributed normally.

$$\begin{aligned}\text{Turbidity removal}(\%) = {} & +76.92 + 43.56A - 22.70B + 6.24C \\ & - 10.11D + 16.21E + 16.76F + 20.07AB - .89AC \\ & + 6.42AD - 10.22AE - 11.61AF + 4.02BC - 6.69BD \\ & + 3.27BE + 12.37BF - 0.8875CD - 3.74CE - 4.69CF \\ & + 6.60DE + 1.99DF + 2.98EF + 7.26A^2 - 62.72B^2 \\ & + 28.96C^2 - 22.38D^2 - 8.02E^2 + 27.12F^2 \end{aligned} \quad (3)$$

EFFECT OF THE MAIN VARIABLES

Effect of initial turbidity and settling time

The experiments were performed to better understand the impact of varied initial turbidity (10–350 NTU) and settling time (10–50 min) on the turbidity removal. The simultaneous effect of the initial turbidity and settling time on the turbidity removal is shown in Figure 2. As can be observed, when the initial turbidity increased from 10 to 350 NTU the removal efficiency of the system increased by more than 99%. On the other hand, minimum residual turbidity was attained at the initial turbidity of 350 NTU. The lower elimination of turbidity at low initial turbidity (10 NTU) may be due to the particle size reduction, which creates smaller flocs with a lower tendency for settling (Camacho *et al.* 2017). Furthermore, Figure 2 shows that the maximum efficiency of 99.14% was achieved at a settling time of 50 min so that when the settling time increased to 50 min, the minimum residual of turbidity (3 NTU) was attained.

Senthil Kumar *et al.* (2016) reported that the Moringa oleifera seeds could eliminate turbidity from underground water. The results completely demonstrated that by increasing the initial turbidity from 50 to 135 NTU, the removal

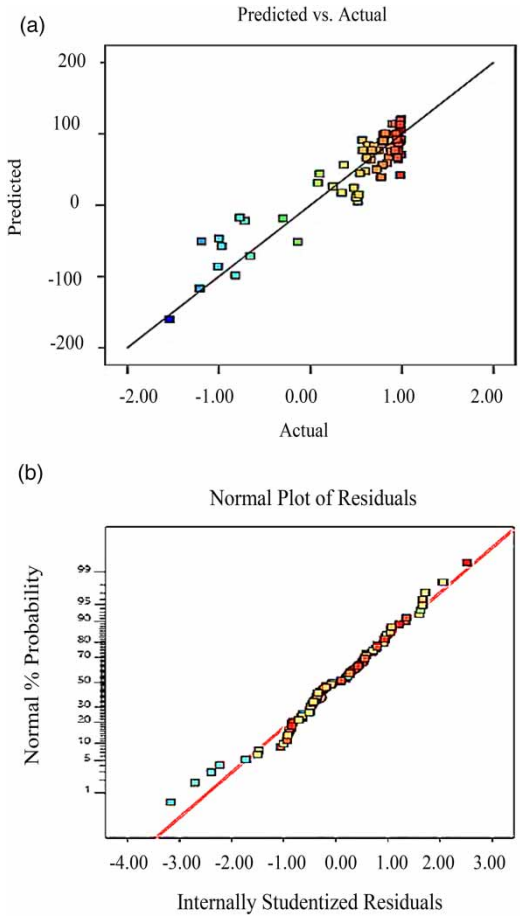

Figure 1 | Predicted vs. actual values plot (a) and normal plot distributions of the residuals (b) for the removal of turbidity.

efficiency increased from 54.67 to 74.28%. It indicates that at higher turbidity concentrations more interaction between coagulants and colloidal particles takes place (Senthil Kumar *et al.* 2016). Ramavandi (2014) used the Plantago ovata as a coagulant to remove turbidity, in which the turbidity varied from 50 to 300 NTU. The study showed that at the first stage of the process with an increase in initial turbidity from 50 to 250 NTU, the turbidity removal efficiency decreased from 99 to 95%, further increase in initial turbidity from 250 to 300 NTU was the cause of increase in the removal efficiency of the process (Ramavandi 2014). Daryabeigi Zand & Hoveidi (2015) compared the efficiency of two commercial coagulants (aluminum sulfate and poly-aluminum chloride) under similar conditions (dosage of 10–20 mg/L, pH 4–8) for treatment of high turbidity (10–1,000 NTU). The results confirmed that initial turbidity

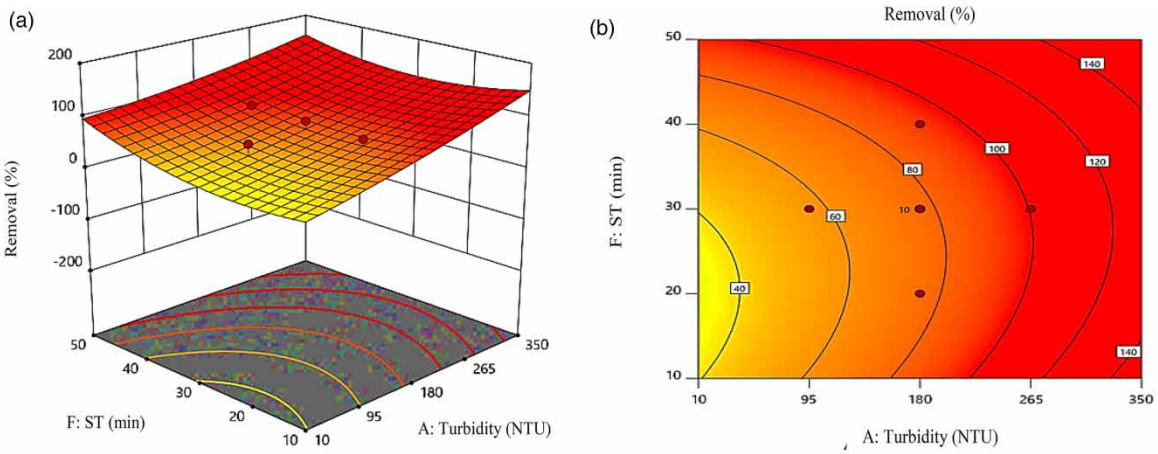

Figure 2 | (a) 3D surface and (b) 2D contour plots showing the simultaneous effect of turbidity and settling time on the removal of turbidity: alum dosage (150 mg/L), rapid mixing (200 rpm), slow mixing (40 rpm) and pH = 7.

had a positive and significant effect on turbidity removal so that when turbidity increased to 500 and 1,000 NTU, the turbidity removal efficiency also remained high (Daryabeigi Zand & Hoveidi 2015).

Altaher *et al.* (2016) represented the turbidity removal of alum with a coagulant aid. The results showed that with increasing settling time, the amount of residual turbidity decreased, indicating that settling time plays a very important role in the CF process (Altaher *et al.* 2016). Similar results by Sasikala & Muthuraman (2017), in which the natural coagulants were used to remove turbidity from surface water, explicitly declared that by increasing settling time in the coagulation process, the turbidity removal efficiency increased (Sasikala & Muthuraman 2017). Also, Mohammed & Shakir (2018) reported that the removal of residual turbidity increased when settling time increased to 20 min.

Effect of pH and coagulant dosage

Generally, one of the most challenging parameters in the CF processes is pH, and the only reliable way to determine the appropriate range of this parameter is by performing laboratory-scale tests (Orooji *et al.* 2016). On the other hand, changing the pH value influences the substance hydrolysis load, and therefore pH optimization is very important to achieve suitable efficiency in CF processes (Al-Husseini *et al.* 2018). In this section, the simultaneous effects of the desired pH (5–9) and coagulant dosage (50–250 mg/L) are discussed. Based on Figure 3, it can be observed that the increase in the pH from 5 to 9 could increase the turbidity removal to 99.14%. In this study, we used alum as a coagulant, and the best removal efficiency occurred at pH 9. It is better to state that the pH range in the alum is between 5.5 and 8.5 (Altaher 2012).

The coagulant dosage can be deemed as one of the operational parameters for determining the optimal conditions of the process (Bazrafshan *et al.* 2015). Moreover, it is necessary to adjust the coagulant dosage because increasing the coagulant dosage may lead to an increase in operating costs, sludge production, shorten filter life, and decrease alkalinity (Ødegaard *et al.* 2010). According to Figure 3, it is clear that when the coagulant dosage was boosted to 250 mg/L, the turbidity removal declined, and the best condition was observed at a low coagulant dosage (50 mg/L). Several studies have shown the effect of pH and coagulant dosage on the CF process. Mohammadi-Moghaddam *et al.* (2015) studied the feasibility of polyaluminum ferric chloride for the treatment of highly turbid water (250 and 500 NTU) and pH value varied from 5 to 11. Their results indicated that increasing pH (more than 9) could result in decreasing the efficiency of the system, therefore, they chose a pH range of 7–8.5 to obtain the minimum residual turbidities (≤0.6 NTU) (Mohammadi-Moghaddam *et al.* 2015). Hussain *et al.* (2019) applied pine cone extract as a natural coagulant for the treatment of turbid water, and the pH value was varied from 2 to 12. Their results showed that by increasing the pH from 2 to 7, the removal efficiency of the process decreased from 75% to almost

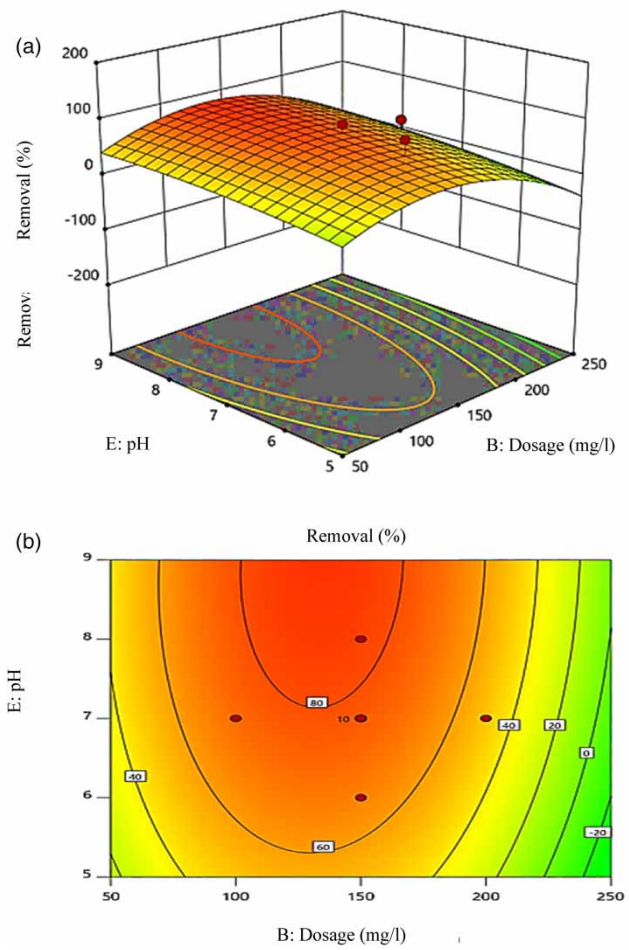

Figure 3 | (a) 3D surface and (b) 2D contour plots showing the simultaneous effect of coagulant dosage and pH on the removal of turbidity at rapid mixing of 200 rpm, slow mixing at 40 rpm and settling time of 30 min.

45%, but with a further increase in pH from 7 to 12, the removal efficiency increased significantly (Hussain *et al.* 2019).

Huang *et al.* (2016) investigated the turbidity removal using a titanium salt family as a coagulant. The results showed that by increasing the coagulant dosage, the efficiency of turbidity removal increased (Huang *et al.* 2016). Chen *et al.* (2015) revealed that when the dosage of coagulant increased, the turbidity removal efficiency was also increased (Chen *et al.* 2015). Chekli *et al.* (2017) used different coagulants for the removal of turbidity and their results demonstrated that by increasing the dosage of coagulants, the removal efficiency of the CF process also increased to 95% (Chekli *et al.* 2017). Dehkordi *et al.* (2017) evaluated the effectiveness of three coagulants including polyaluminum chloride, alum, and ferric chloride, with a coagulant aid to remove turbidity in slopes ranging from 50 to over 20,000 NTUs. The results demonstrated that the removal efficiency of the process increased as coagulant dosage increased (Dehkordi *et al.* 2017).

Effect of mixing

Rapid mixing is an important parameter that has been investigated in CF processes in which chemical coagulants are combined with freshwater to promote particle destabilization (Ramphal & Sibiya 2014). It is better to mention that rapid mixing in a shorter time increases the remaining turbidity and creates larger flocs (BinAhmed *et al.* 2015). On the other hand, a high value of G, which is called the rapid mixing phase in the CF processes, usually facilitates the suitable dispersion of the added coagulant to the suspension and also improves contact between the particles, the soluble materials, and the coagulant molecules (Sheng *et al.* 2006).

The primary purpose of mixing is to keep particles in the suspended state, additionally, slow mixing can provide a velocity gradient for collisions between particles larger than 1 μm (Zhang *et al.* 2013). Furthermore, the slow mixing speed must be sufficient to maintain suspending particles without floc breakage (Rossini *et al.* 1999). Based on the obtained results (Figure 4), it was concluded that when rapid mixing increased to 280 rpm, the efficiency of turbidity removal improved, and maximum efficiency was 99.14%. Besides, as observed, by increasing the slow mixing from 30 to 50 rpm, the efficiency of turbidity removal increased slightly. Rossini *et al.* (1999) investigated the effect of the rapid mixing parameter in the CF process, and the results showed that the high value of the velocity gradient in the rapid mixing could result in creating lower residual turbidity (Rossini *et al.* 1999). Kan *et al.* (2002) tested the effects of varied rapid mixing intensity (25, 80, 200, 350, and 600 s^{-1}) by PACl. The results confirmed that when rapid mixing intensity increased, the turbidity removal decreased (Kan *et al.* 2002). The results of a study by Zhang *et al.* (2013) verified that when the slow-mixing duration is within a certain range, such as $t < 15$ min at $G = 15$ or 38 s^{-1}, the residual

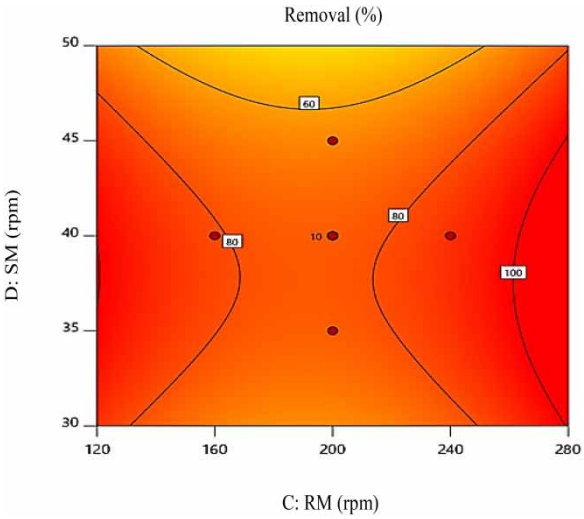

Figure 4 | 2D contour plot showing the simultaneous effect of rapid mixing and slow mixing on the removal of turbidity (initial turbidity of 180 NTU, alum dosage of 150 mg/L, pH of 7, and settling time of 30 min).

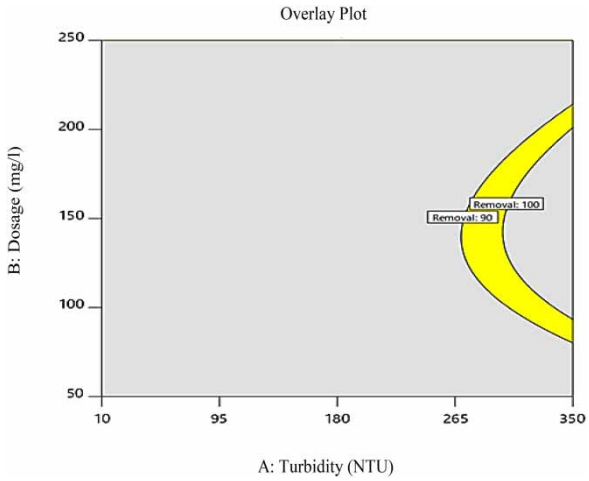

Figure 5 | Optimum overlay conversion contour plot.

turbidity declined with slow-mixing duration. However, when increasing the slow-mixing duration such as $t > 15$ min at $G = 15$ or 38 s^{-1}, the residual turbidity increases, even when the G value is as low as 4 s^{-1} (Zhang *et al.* 2013).

Optimization

The empirical results were optimized by Design-Expert software to produce an overlay plot. The amount of residual turbidity and alum dosage on the turbidity removal as responses were optimized (Figure 5). As can be seen, the optimal condition of the experiments was obtained under rapid mixing of 191 rpm, slow mixing of 43 rpm, pH 5.5, and settling time of 36 min, and high removal efficiency was between 90 and 100%.

CONCLUSIONS

In this study, a high concentration of turbidity (10–350 NTU) was removed by alum in batch experiments using the CF process. To optimize the impact of independent variables on the CF system, CCD based RSM was used. The results of the research revealed that the initial concentration of turbidity had the most significant role in the system so that 99.14% turbidity was eliminated at 350 NTU. Furthermore, under the optimum conditions of rapid mixing (191 rpm), slow mixing (43 rpm), pH (5.5), and also settling time (36 min), the removal of turbidity varied between 90 and 100%. This study highlighted that the CF process is the most reliable chemical method for removing highly turbid water.

ACKNOWLEDGEMENTS

The authors hereby express their gratitude to the Water and Wastewater Company of Kermanshah Province for financial support (Grant number: 129/95/21868), and Kermanshah University of Medical Sciences for supplying laboratory facilities.

DATA AVAILABILITY STATEMENT

All relevant data are included in the paper or its Supplementary Information.

REFERENCES

Aboubaraka, A. E., Aboelfetoh, E. F. & Ebeid, E.-Z. M. 2017 Coagulation effectiveness of graphene oxide for the removal of turbidity from raw surface water. *Chemosphere* **181**, 738–746.

Agbovi, H. K. & Wilson, L. D. 2019 Optimisation of orthophosphate and turbidity removal using an amphoteric chitosan-based flocculant–ferric chloride coagulant system. *Environ. Chem.* **16** (8), 599–612.

Al-Husseini, T. R., Ghawi, A. H. & Ali, A. H. 2018 Performance of hydraulic jump rapid mixing for enhancement of turbidity removal from synthetic wastewater: a comparative study. *J. Water Process Eng.* **30** (12), 105–120.

Almasi, A., Navazeshkhaa, F. & Mousavi, S. A. 2017 Biosorption of lead from aqueous solution onto Nasturtium officinale: performance and modeling. *Desal. Water Treat.* **65**, 443–450.

Altaher, H. 2012 The use of chitosan as a coagulant in the pre-treatment of turbid sea water. *J. Hazard. Mater.* **233**, 97–102.

Altaher, H., Tarek, E. & Abubeah, R. 2016 An agricultural waste as a novel coagulant aid to treat high turbid water containing humic acids. *Glob. Nest J.* **18** (2), 279–290.

Ang, W., Mohammad, A., Benamor, A. & Hilal, N. 2016 Chitosan as natural coagulant in hybrid coagulation-nanofiltration membrane process for water treatment. *J. Environ. Chem. Eng.* **4** (4), 4857–4862.

Antov, M. G., Šćiban, M. B., Prodanović, J. M., Kukić, D. V., Vasić, V. M., Đorđević, T. R. & Milošević, M. M. 2018 Common oak (Quercus robur) acorn as a source of natural coagulants for water turbidity removal. *Ind. Crops Prod.* **117**, 340–346.

Aydar, A. Y. 2018 Utilization of response surface methodology in optimization of extraction of plant materials. In: *Statistical Approaches with Emphasis on Design of Experiments Applied to Chemical Processes*. IntechOpen, 157–169.

Azimi, S. C., Shirini, F. & Pendashteh, A. 2019 Evaluation of COD and turbidity removal from woodchips wastewater using biologically sequenced batch reactor. *Process Saf. Environ. Prot.* **128**, 211–227.

Baghvand, A., Zand, A. D., Mehrdadi, N. & Karbassi, A. 2010 Optimizing coagulation process for low to high turbidity waters using aluminum and iron salts. *Am. J. Environ. Sci.* **6** (5), 442–448.

Baruth, E. E. 2005 *Water Treatment Plant Design*, 4th edn. McGraw-Hill, New York.

Bazrafshan, E., Mostafapour, F. K., Ahmadabadi, M. & Mahvi, A. H. 2015 Turbidity removal from aqueous environments by Pistacia atlantica (Baneh) seed extract as a natural organic coagulant aid. *Desal. Water Treat.* **56** (4), 977–983.

BinAhmed, S., Ayoub, G., Al-Hindi, M. & Azizi, F. 2015 The effect of fast mixing conditions on the coagulation–flocculation process of highly turbid suspensions using liquid bittern coagulant. *Desal. Water Treat.* **53** (12), 3388–3396.

Camacho, F. P., Sousa, V. S., Bergamasco, R. & Teixeira, M. R. 2017 The use of Moringa oleifera as a natural coagulant in surface water treatment. *Chem. Eng. J.* **313**, 226–237.

Chekli, L., Eripret, C., Park, S., Tabatabai, S., Vronska, O., Tamburic, B., Kim, J. & Shon, H. 2017 Coagulation performance and floc characteristics of polytitanium tetrachloride (PTC) compared with titanium tetrachloride (TiCl4) and ferric chloride (FeCl3) in algal turbid water. *Separ. Purif. Technol.* **175**, 99–106.

Chen, W., Zheng, H., Zhai, J., Wang, Y., Xue, W., Tang, X., Zhang, Z. & Sun, Y. 2015 Characterization and coagulation–flocculation performance of a composite coagulant: poly-ferric-aluminum-silicate-sulfate. *Desal. Water Treat.* **56** (7), 1776–1786.

Corral Bobadilla, M., Lorza, R. L., Escribano García, R., Somovilla Gómez, F. & Vergara González, E. P. 2019 Coagulation: determination of key operating parameters by multi-response surface methodology using desirability functions. *Water* **11** (2), 398.

Daryabeigi Zand, A. & Hoveidi, H. 2015 Comparing aluminium sulfate and poly-aluminium chloride (PAC) performance in turbidity removal from synthetic water. *J. Appl. Biotechnol. Rep.* **2** (3), 287–292.

Dehkordi, D. K., Kashkuli, H. A., Mohsenifar, K. & Sadeghi-Mianroudi, M. 2017 Assessment of coagulants efficiency in water treatment of Karoun River, Jundishapur. *J. Health Sci.* **9** (3), e37193.

Gagnon, C., Grandjean, B. P. & Thibault, J. 1997 Modelling of coagulant dosage in a water treatment plant. *Artif. Intell. Eng.* **11** (4), 401–404.

Gasemloo, S., Khosravi, M., Sohrabi, M. R., Dastmalchi, S. & Gharbani, P. 2019 Response surface methodology (RSM) modeling to improve removal of Cr (VI) ions from tannery wastewater using sulfated carboxymethyl cellulose nanofilter. *J. Clean. Prod.* **208**, 736–742.

Gobena, B., Adela, Y. & Alemayehu, E. 2018 Evaluation of mix-chemical coagulants in water purification process. *Int. J. Eng. Res. Technol.* **7** (01), 431–435.

Hajiali, A. & Pirumyan, G. P. 2014 Evaluation of turbidity and color removal in treatment of wastewater containing resistant pollutants with ozonation. *IERI Procedia* **9**, 8–12.

Huang, X., Gao, B., Rong, H., Yue, Q., Zhang, Y. & Teng, P. 2015 Effect of using polydimethyldiallylammonium chloride as coagulation aid on polytitanium salt coagulation performance, floc properties and sludge reuse. *Separ. Purif. Technol.* **143**, 64–71.

Huang, X., Zhao, Y., Gao, B., Sun, S., Wang, Y., Li, Q. & Yue, Q. 2016 Polyacrylamide as coagulant aid with polytitanium sulfate in humic acid-kaolin water treatment: effect of dosage and dose method. *J. Taiwan Inst. Chem. Eng.* **64**, 173–179.

Hussain, S., Ghouri, A. S. & Ahmad, A. 2019 Pine cone extract as natural coagulant for purification of turbid water. *Heliyon* **5** (3), e01420.

Kan, C., Huang, C. & Pan, J. R. 2002 Coagulation of high turbidity water: the effects of rapid mixing. *J. Water Supply Res. Technol. Aqua* **51** (2), 77–85.

Kim, C. M. & Parnichkun, M. 2017 Prediction of settled water turbidity and optimal coagulant dosage in drinking water treatment plant using a hybrid model of k-means clustering and adaptive neuro-fuzzy inference system. *Appl. Water Sci.* **7** (7), 3885–3902.

Kumari, M. & Gupta, S. K. 2020 A novel process of adsorption cum enhanced coagulation-flocculation spiked with magnetic nanoadsorbents for the removal of aromatic and hydrophobic fraction of natural organic matter along with turbidity from drinking water. *J. Clean. Prod.* **244**, 118899.

Lim, B.-C., Lim, J.-W. & Ho, Y.-C. 2018 Garden cress mucilage as a potential emerging biopolymer for improving turbidity removal in water treatment. *Process Saf. Environ. Prot.* **119**, 233–241.

Mohammadi-Moghaddam, F., Mahdavi, M., Hajizadeh, Y., Tashauoei, H. R., Ataeifar, H. & Ebrahimi, A. 2015 Treatment of highly turbid water by polyaluminum ferric chloride (PAFCL). *Arch. Hyg. Sci.* **4** (4), 208–216.

Mohammed, T. J. & Shakir, E. 2018 Effect of settling time, velocity gradient, and camp number on turbidity removal for oilfield produced water. *Egypt. J. Petrol.* **27** (1), 31–36.

Momeni, M. M., Kahforoushan, D., Abbasi, F. & Ghanbarian, S. 2018 Using chitosan/CHPATC as coagulant to remove color and turbidity of industrial wastewater: optimization through RSM design. *J. Environ. Manage.* **211**, 347–355.

Mousavi, S. A. & Ibrahim, S. 2016 Application of response surface methodology (RSM) for analyzing and modeling of nitrification process using sequencing batch reactors. *Desal. Water Treat.* **57** (13), 5730–5739.

Mousavi, S., Mehralian, M., Khashij, M. & Parvaneh, S. 2017 Methylene Blue removal from aqueous solutions by activated carbon prepared from N. microphyllum (AC-NM): RSM analysis, isotherms and kinetic studies. *Glob. Nest J.* **19** (4), 697–705.

Mousavi, S. A., Almasi, A., Navazeshkha, F. & Falahi, F. 2019 Biosorption of lead from aqueous solutions by algae biomass: optimization and modeling. *Desal. Water Treat.* **148**, 229–237.

Muyibi, S. & Alfugara, A. 2003 Treatment of surface water with Moringa Oleifera seed extract and alum – a comparative study using a pilot scale water treatment plant. *Int. J. Environ. Stud.* **60** (6), 617–626.

Nadarajan, R., Bakar, W. A. W. A., Ali, R. & Ismail, R. 2018 Photocatalytic degradation of 1, 2-dichlorobenzene using immobilized TiO2/SnO2/WO3 photocatalyst under visible light: application of response surface methodology. *Arab. J. Chem.* **11** (1), 34–47.

Nayeri, D., Mousavi, S. A., Fatahi, M., Almasi, A. & Khodadoost, F. 2019 Dataset on adsorption of methylene blue from aqueous solution onto activated carbon obtained from low cost wastes by chemical-thermal activation – modelling using response surface methodology. *Data in Brief.* **25**, 104036.

Noordin, M. Y., Venkatesh, V. C., Sharif, S., Elting, S. & Abdullah, A. 2004 Application of response surface methodology in describing the performance of coated carbide tools when turning AISI 1045 steel. *J. Mater. Process. Technol.* **145** (1), 46–58.

Ødegaard, H., Østerhus, S., Melin, E. & Eikebrokk, B. 2010 NOM removal technologies – Norwegian experiences. *Drinking Water Eng. Sci.* **3** (1), 1–9.

Orooji, N., Takdastan, A., Eslami, A., Kargari, A. & Raeesi, G. 2016 Study of the chitosan performance in conjunction with polyaluminum chloride in removing turbidity from Ahvaz water treatment plant. *Desal. Water Treat.* **57** (43), 20,332–20,339.

Ozairi, N., Mousavi, S. A., Samadi, M. T., Seidmohammadi, A. & Nayeri, D. 2020 Removal of fluoride from water using coagulation-flocculation process: a comparative study. *Desal. Water Treat.* **180**, 265–270.

Park, W.-I., Jeong, S., Im, S.-J. & Jang, A. 2020 High turbidity water treatment by ceramic microfiltration membrane: fouling identification and process optimization. *Environ. Technol. Innov.* **17**, 1–10.

Ramavandi, B. 2014 Treatment of water turbidity and bacteria by using a coagulant extracted from Plantago ovata. *Water Resour. Ind.* **6**, 36–50.

Ramphal, S. & Sibiya, S. M. 2014 Optimization of time requirement for rapid mixing during coagulation using a photometric dispersion analyzer. *Proc. Eng.* **70**, 1401–1410.

Rossini, M., Garrido, J. G. & Galluzzo, M. 1999 Optimization of the coagulation–flocculation treatment: influence of rapid mix parameters. *Water Res.* **33** (8), 1817–1826.

Sasikala, S. & Muthuraman, G. 2017 Turbidity removal from surface water by natural coagulants and its potential application. *Iran. J. Energy Environ.* **8** (1), 61–66.

Senthil Kumar, P., Centhil, V., Kameshwari, R., Palaniyappan, M., Kalaivani, V. D. & Pavithra, K. G. 2016 Experimental study on parameter estimation and mechanism for the removal of turbidity from groundwater and synthetic water using Moringa oleifera seed powder. *Desal. Water Treat.* **57** (12), 5488–5497.

Shahbazi, D., Mousavi, S. A. & Nayeri, D. 2020 Low-cost activated carbon: characterization, decolorization, modeling, optimization and kinetics. *Int. J. Environ. Sci. Technol.* **17** (1), 3935–3946.

Sheng, W.-Y., Peng, X., Lee, D. & Su, A. 2006 Coagulation of particles through rapid mixing. *Drying Technol.* **24** (10), 1271–1276.

Singh, K. P. & Gupta, S. 2012 Artificial intelligence based modeling for predicting the disinfection by-products in water. *Chemometr. Intell. Lab. Syst.* **114**, 122–131.

Singh, B. & Kumar, P. 2020 Pre-treatment of petroleum refinery wastewater by coagulation and flocculation using mixed coagulant: optimization of process parameters using response surface methodology (RSM). *J. Water Process Eng.* **36**, 101317.

Specht, D. F. 1991 A general regression neural network. *IEEE Trans. Neural Netw.* **2** (6), 568–576.

Usefi, S. & Asadi-Ghalhari, M. 2019 Modeling and optimization of the coagulation–flocculation process in turbidity removal from aqueous solutions using rice starch. *Pollution* **5** (3), 623–636.

Zangeneh, H., Zinatizadeh, A. A. L. & Feyzi, M. 2016 Degradation of linear alkyl benzene using an immobilized nano tio2 photocatalytic reactor: process analysis and modeling. *Clean Soil Air Water* **44** (1), 78–88.

Zhang, Z., Dan, L., Dandan, H., Duo, L., Xiaojing, R., Cheng, Y. & Zhaokun, L. 2013 Effects of slow-mixing on the coagulation performance of polyaluminum chloride (PACI). *Chin. J. Chem. Eng.* **21** (3), 318–323.

Zhang, Z., Jing, R., He, S., Qian, J., Zhang, K., Ma, G., Chang, X., Zhang, M. & Li, Y. 2018 Coagulation of low temperature and low turbidity water: adjusting basicity of polyaluminum chloride (PAC) and using chitosan as coagulant aid. *Separ. Purif. Technol.* **206**, 131–139.

Zhao, S., Gao, B., Li, X. & Dong, M. 2012 Influence of using Enteromorpha extract as a coagulant aid on coagulation behavior and floc characteristics of traditional coagulant in Yellow River water treatment. *Chem. Eng. J.* **200**, 569–576.

First received 9 June 2020; accepted in revised form 23 August 2020. Available online 22 October 2020